High resolution analysis of the v(12) and v(17) fundamental bands of acrolein, CH2CHCHO, in the 600 cm(−1) region

ARTICLE *in* JOURNAL OF MOLECULAR SPECTROSCOPY · MARCH 2007

Impact Factor: 1.48 · DOI: 10.1016/j.jms.2007.01.005

Available online at www.sciencedirect.com
ScienceDirect
Journal of Molecular Spectroscopy 242 (2007) 31–38
Journal of MOLECULAR SPECTROSCOPY
www.elsevier.com/locate/jms

High resolution analysis of the v_{12} and v_{17} fundamental bands of acrolein, CH_2CHCHO, in the 600 cm^{-1} region

A.R.W. McKellar [a,*], D.W. Tokaryk [b], Li-Hong Xu [c], D.R.T. Appadoo [d], T. May [d]

[a] Steacie Institute for Molecular Sciences, National Research Council of Canada, Ottawa, Ont., Canada K1A 0R6
[b] Department of Physics and Centre for Laser, Atomic, and Molecular Sciences, University of New Brunswick, Fredericton, NB, Canada E3B 5A3
[c] Department of Physical Sciences and Centre for Laser, Atomic, and Molecular Sciences, University of New Brunswick, Saint John, NB, Canada E2L 4L5
[d] Canadian Light Source, 101 Perimeter Road, University of Saskatchewan, Saskatoon, Sask., Canada S7N 0X4

Received 13 December 2006
Available online 1 February 2007

Abstract

Synchrotron radiation from the new Canadian Light Source facility has been used to obtain a high resolution (0.0012 cm^{-1}) absorption spectrum of acrolein vapor in the 550–660 cm^{-1} region. Almost 2000 transitions have been included in a detailed analysis of the v_{12} (~564 cm^{-1}) and v_{17} (~593 cm^{-1}) fundamental bands which yielded precise values for the band origins, rotational and centrifugal distortion parameters. The analysis included the *a*- and *b*-type Coriolis interactions connecting v_{12} and v_{17}, as well as an *a*-type Coriolis interaction between v_{17} and a "dark" perturbing state, identified as $4v_{18}$. We believe that this is the first high resolution infrared study of acrolein.

Keywords: Acrolein; Propenol; Infrared; Synchrotron; Coriolis

1. Introduction

Acrolein (propenol) is a fundamental 8-atomic molecule which is of interest as a possible interstellar species [1], a combustion byproduct [2], a component of photochemical smog, and a potent respiratory irritant [3,4]. The *trans* rotamer of acrolein is the lowest energy form and has been the subject of most spectroscopic investigations. A fairly comprehensive study of the pure rotational microwave spectrum of acrolein in its ground vibrational state was reported in 1975 by Winnewisser et al. [5], building on earlier microwave results [6,7]. Vibrational analyses have been made on the basis of electronic spectra [8–12] and medium-resolution infrared spectra [13], and definitive results are given in a paper by Hamada et al. [14] which contains references to earlier work on acrolein. An extensive lower resolution (0.3 cm^{-1}) study of the far-infrared (100–400 cm^{-1}) spectrum of acrolein by Cole and Green [15] is also directly relevant to the present work.

We are not aware of any previous high resolution infrared studies of acrolein. In the present paper, we describe a detailed analysis of the Coriolis-coupled v_{12} and v_{17} fundamental bands of CH_2CHCHO in the 550–660 cm^{-1} region. v_{17} is the vinyl CH out-of-plane wagging mode, which gives rise to a strong *c*-type band centered at about 593 cm^{-1}, and v_{12} is the CCO bending mode, which gives rise to a weaker *a*-type band at about 564 cm^{-1} [14]. The analysis includes almost 2000 transitions with values of (J', K'_a) ranging up to (45, 20) for v_{17} and (37, 16) for v_{12}. We obtain precise band origins, excited state rotational and centrifugal distortion parameters, and Coriolis interaction parameters. In addition, we identify a perturbation of v_{17} by the $4v_{18}$ state and thus indirectly gain some information on this overtone state, which is located at about 622 cm^{-1}.

2. Experimental details

A room temperature absorption spectrum of acrolein in the 550–700 cm^{-1} region was obtained with near Doppler-limited resolution at the Canadian Light Source (CLS)

* Corresponding author. Fax: +1 613 991 2648.
E-mail address: robert.mckellar@nrc-cnrc.gc.ca (A.R.W. McKellar).

0022-2852/$ - see front matter © 2007 Elsevier Inc. All rights reserved.
doi:10.1016/j.jms.2007.01.005

using synchrotron radiation as the infrared continuum source. We used a Bruker IFS 125HR Fourier transform spectrometer operating with an entrance aperture of 1.5 mm and a nominal resolution of 0.0012 cm^{-1}. It was fitted with a KBr beamsplitter and a 77 K broadband MCT detector. Acrolein vapor at a pressure of 0.3 Torr was contained in a 0.3 m multiple traversal cell set for an absorption path of 8.4 m. The final spectrum was the result of an average of 414 interferograms involving about 35 h of acquisition time.

The CLS facility consists of a 200–300 MeV electron linac, a booster ring, and a storage ring with a circumference of 171 m operating at 2.9 GeV. The average electron beam current for the present results was about 172 mA. Synchrotron light sources were originally used mostly for the ultraviolet and *x*-ray wavelength regions, but more recently they have proven their value as infrared (IR) sources. Most synchrotron IR beamlines are used for mid-IR spectromicroscopy, taking advantage of the high brightness of synchrotron radiation to acquire two-dimensional spectral maps of condensed phase samples (e.g. biological tissue) with high spatial resolution and modest ($\sim$1 cm^{-1}) spectral resolution. However, a bright source is also advantageous for high spectral resolution, since the entrance aperture of a Fourier transform spectrometer must decrease as resolution increases. High resolution gas-phase IR spectroscopy using synchrotron radiation was pioneered by Bengt Nelander at MAXLab in Lund, Sweden [16,17], where a number of results in the far IR region have been obtained [18–21]. Promising results have also been reported from the LURE synchrotron [22], and gas-phase IR beamlines are under construction or planned at a number of other facilities (SOLEIL, Australian Synchrotron, Swiss Light Source, Singapore Synchrotron Light Source).

The present results were obtained during the commissioning phase of the CLS Far Infrared Beamline. At this stage, excess noise in the synchrotron IR signal remains a significant challenge. This noise arises mainly from mechanical vibrations in the chain of mirrors which transfer the IR radiation to the spectrometer from its origin at a bending magnet in the storage ring. In spite of these difficulties, the signal-to-noise ratio using synchrotron radiation was already better in the 600 cm^{-1} region than could be obtained with the spectrometer's internal thermal (globar-type) source. The situation is illustrated in Fig. 1, which shows a small portion of the present acrolein spectrum near 611 cm^{-1} (this is the $^{r}Q_6(J)$ branch of the ν_{17} band). The top trace in Fig. 1 is the final synchrotron result analyzed here, the center trace is a preliminary synchrotron result, and the lower trace was obtained with the internal globar source. Note that the noise levels in the lower two traces are similar, but that the globar spectrum involved

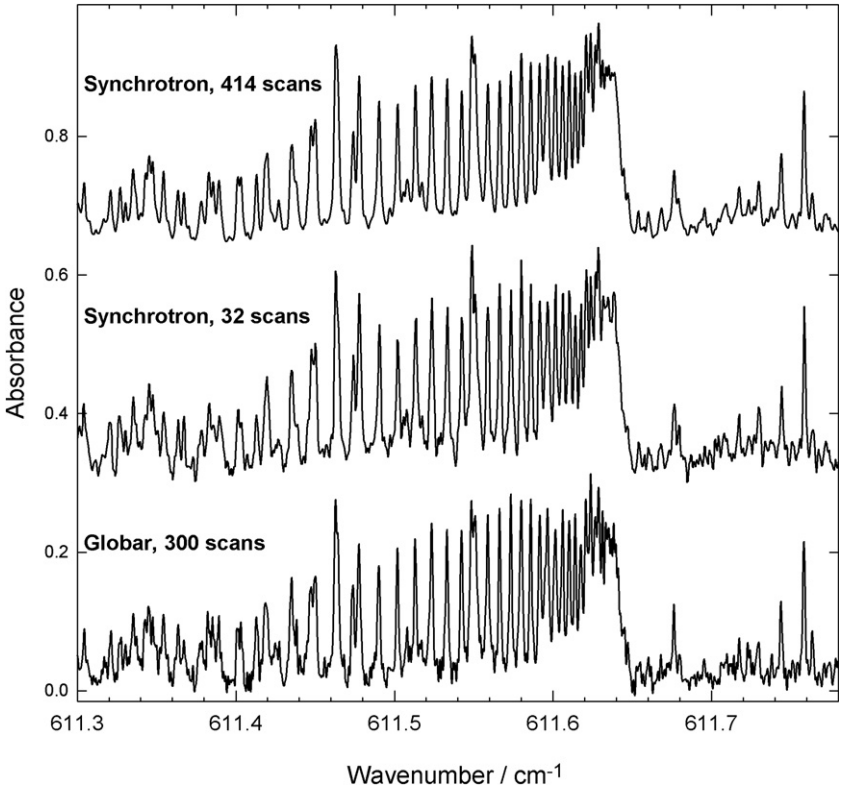

Fig. 1. Part of the observed spectrum of acrolein comparing the signal-to-noise ratios obtained with the spectrometer's internal thermal ('globar') source and with synchrotron radiation with different numbers of scans. The synchrotron gave 3–4 times better signal-to-noise in this spectral region. This translated into about an order of magnitude reduction in signal acquisition time, as shown by the similar noise levels in the two lower traces.

almost an order of magnitude more data acquisition time, a reflection of 3–4 times better signal-to-noise ratio from the synchrotron.

3. Results and analysis

3.1. Introduction and theory

Acrolein is a planar near-prolate ($A > B \approx C$) asymmetric rotor. It belongs to the C_s point group, with the only symmetry element being its planarity, and has both *a*- and *b*-type permanent dipole moments (3.06 and 0.54 D, respectively) [6,7]. In-plane vibrations have A' symmetry and give rise to hybrid bands which may have *a*- and/or *b*-type transitions, while out-of-plane fundamental vibrations with A'' symmetry give rise to *c*-type bands. In this paper, we deal with the ν_{12} (A', CCO bend) and ν_{17} (A'', vinyl CH wag) fundamentals. We also encounter the "dark" perturbing state $4\nu_{18}$, which has A' symmetry since it is an even overtone of the ν_{18} (out-of-plane C–C torsion) vibration.

The analysis and fitting of the spectrum were made using the *A*-reduced Hamiltonian of Watson [23], implemented in a computer program based on that used previously in studies of HFCO [24] and other molecules, now generalized to include three interacting vibrational states. The vibrationally off-diagonal matrix elements which were included in the final fit are listed here

$$\begin{aligned}
\langle v_{12},k|H|v_{17},k\rangle &= G_a(12,17)k\\
\langle v_{12},k|H|v_{17},k\pm1\rangle &= \tfrac{1}{2}[G_b(12,17)+Z_3(2k\pm1)][J(J+1)\\
&\quad -k(k\pm1)]^{\frac{1}{2}}\\
\langle v_{12},k|H|v_{17},k\pm2\rangle &= \pm\tfrac{1}{2}Z_1\{[J(J+1)-k(k\pm1)]\\
&\quad \times[J(J+1)-(k\pm1)(k\pm2)]\}^{\frac{1}{2}}\\
\langle v_{17},k|H|4v_{18},k\rangle &= [G_a(17,18^4)+Z_5J(J+1)]k. \qquad (1)
\end{aligned}$$

Here G_a and G_b are the *a*- and *b*-type Coriolis interaction parameters, and Z_1, Z_3, and Z_5 are higher-order terms [24]. These *G* parameters are related to the dimensionless Coriolis zeta parameters by expressions such as $G_a(12,17) = 2A\zeta^a_{12,17}$. During the assignment phase of the analysis, we also made extensive use of the JB95 simulation program [25] which allows the observed and calculated spectra to be displayed in an interactive environment.

3.2. Initial assignments

A good low resolution overview of the spectrum of acrolein in the 550–660 cm^{-1} region is shown in Fig. 2 of Ref. [14]. Our observed spectrum, with much higher resolution, was tremendously dense and overlapped, with "wall-to-wall" lines. Fortunately for us, Hamada et al. [14] had already assigned much of the K_a-structure of the ν_{17} fundamental, particularly in the region above about 600 cm^{-1} which is relatively clear and open. So we could immediately

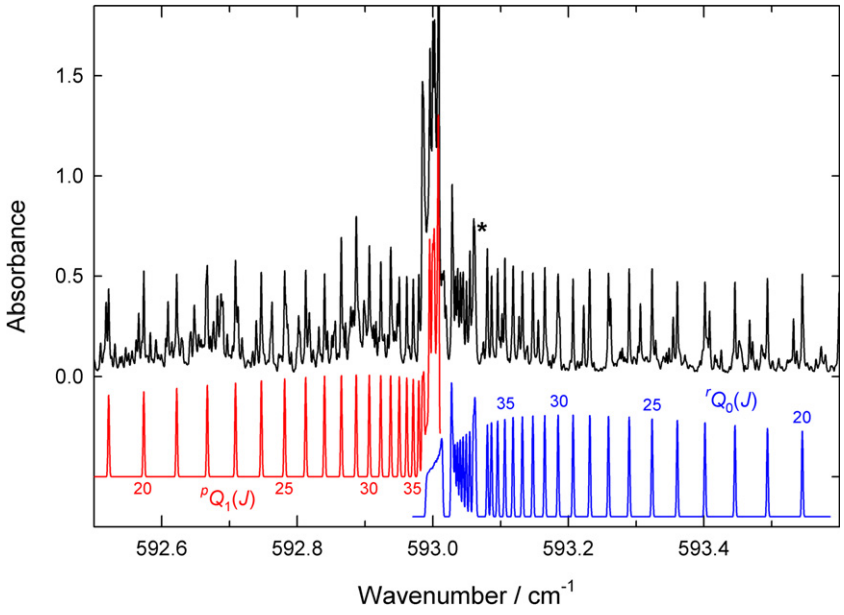

Fig. 2. Upper trace: observed spectrum of acrolein in the region of the ν_{17} band origin. The intense feature at 593.0 cm^{-1} is formed by the merging of the $^pQ_1$ and $^rQ_0$ branches at higher *J*-values, as illustrated by the simulated spectra in the lower two traces. The small gap at 593.07 cm^{-1} indicated by the asterisk is due to a perturbation of $K_a = 1$ levels of ν_{17} by $K_a = 4$ levels of ν_{12} (see Section 4.1). (For interpretation of color mentioned in this figure the reader is referred to the web version of the article.)

begin by assigning ${}^{r}Q_{K_a}(J)$ and ${}^{r}R_{K_a}(J)$ transitions of ν_{17} with good confidence for $K_a \approx 4$–7 in the range of J-values where asymmetry doubling was negligible. In order to move to lower values of K_a where the asymmetry doubling was significant, we tackled the region around 593 cm^{-1} where the strongest single feature in the spectrum is located. This feature, located very close to the ν_{17} band origin, is illustrated in Fig. 2. It is formed by the merging of the ${}^{p}Q_1(J)$ and ${}^{r}Q_0(J)$ branches at high J-values in the "oblate limit" where the $(J, K_a, K_c) = (J, 0, J)$ and $(J, 1, J)$ levels become nearly degenerate. After a small amount of trial and error, it was possible to establish the correct numbering for these two series, and to continue on to other branches with $K_a = 1$, 2, and 3.

The ν_{17} band was thus relatively easy to assign in many regions, but ν_{12} posed more difficulties because it is somewhat weaker and partly overlapped by ν_{17}. As well, it turns out that ν_{12} is predominantly *a*-type, and hence more compact and congested. The *b*-type transitions of ν_{12} were too weak to be clearly identified. But with persistence, and the aid of the JB95 simulation program mentioned above, it was possible to achieve a secure assignment of ν_{12}. The ${}^{q}Q$-branch region of ν_{12} near the band origin was also helpful, and is illustrated in Fig. 3. This region is so highly congested that individual lines could not be used in the fit, but it was still valuable for estimating the effective band origins of the various K_a stacks. [Note that the simulations in Fig. 3 and elsewhere use exact calculated line positions (including Coriolis interactions), and approximate intensities (neglecting such interactions).]

3.3. Fitting the data

The assignments proceeded quickly once a reasonable range of transitions had been assigned for the ν_{12} and ν_{17} bands and preliminary parameters had been determined. However, some perturbations in ν_{17} were noted that could not be explained by the interaction with ν_{12}. In particular, there was a sharp local perturbation of the ν_{17} $K'_a = 13$ levels at $J' = 30$. More generally the levels with $K'_a < 13$ were slightly lower in energy than expected and those with $K'_a > 13$ were slightly higher. These and other perturbations are discussed in detail below.

We found that the particular effect noted around $K'_a = 13$ of ν_{17} could be nicely explained by a Coriolis interaction with the torsional overtone state $4\nu_{18}$. Even though transitions to $4\nu_{18}$ from the ground state have not been observed, we still know a fair amount about it, because three pure rotational microwave transitions within $4\nu_{18}$ were measured by Cherniak and Costain [7]. Moreover, its vibrational origin was estimated to be about 624 cm^{-1} by Cole and Green [15], based on their band contour simulations of the torsional fundamental region (~160 cm^{-1}).

Our final fit of the ν_{12} and ν_{17} bands included about 1960 infrared transitions, of which about 260 were given reduced weights due to their weakness and/or blended nature. About 670 of the transitions involved the weaker ν_{12} band. The vast majority of the ν_{17} band lines in the fit come from the less crowded region above 593 cm^{-1} and involve $\Delta K_a = +1$ transitions from the ${}^{r}Q$ and ${}^{r}R$

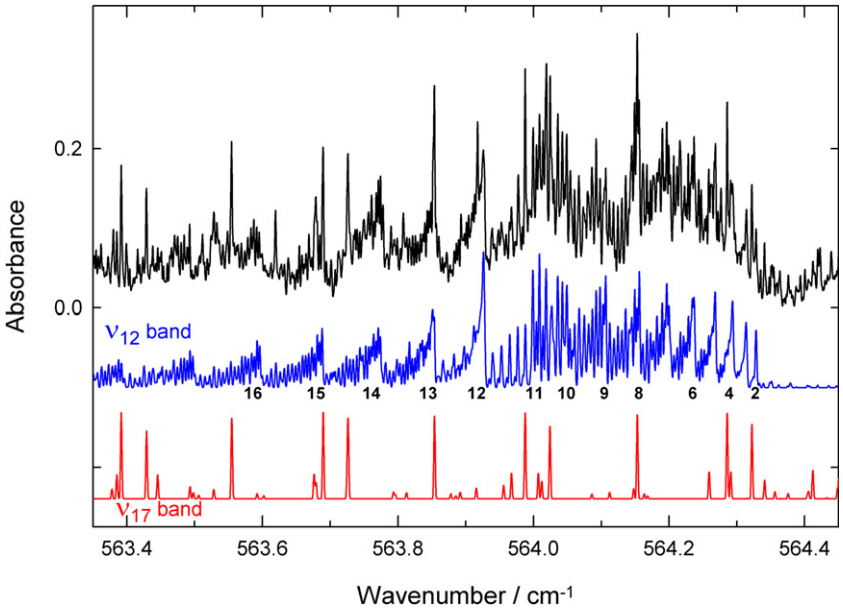

Fig. 3. Upper trace: observed spectrum of acrolein in the region of the ν_{12} band origin. The middle and lower traces show the simulated contributions from the ν_{12} and ν_{17} bands, respectively. The numbers below the ν_{12} simulation indicate K_a-values for the ${}^{q}Q$ sub-branch origins: most of these sub-branches are red-degraded, except for $K_a = 11$ which is blue-degraded, leading to a gap at 563.95 cm^{-1} (see Section 4.1). (For interpretation of color mentioned in this figure the reader is referred to the web version of the article.)

Table 1
Spectroscopic parameters for acrolein (in cm^{-1})[a]

	v_{12}	v_{17}	$4v_{18}$	Ground state[b]
v_0	564.3404(1)	593.0793(1)	621.958(16)	
A	1.5789146(15)	1.5768182(12)	1.384325(23)	1.57954976
B	0.1553289(44)	0.1552016(44)	0.1562836(42)	0.155424164
C	0.14136381(15)	0.14150373(10)	0.1436751(42)	0.141520893
$10^5 \times \Delta_K$	1.23410(33)	1.18322(26)	−8.303(57)	1.20053
$10^7 \times \Delta_{JK}$	−3.2434(74)	−2.8887(20)	−2.92953	−2.92953
$10^8 \times \Delta_J$	3.4938(71)	3.5101(30)	3.47417	3.47417
$10^7 \times \delta_K$	2.18(17)	2.09(10)	1.9342	1.9342
$10^9 \times \delta_J$	3.855(63)	3.917(33)	3.99773	3.99773
$10^{10} \times H_K$		−7.827(49)		
$G_a(12,17)$	0.251076(75)			
$G_b(12,17)$	0.0454(14)			
$10^5 \times Z_1(12,17)$	−6.039(37)			
$10^4 \times Z_3(12,17)$	−4.29(68)			
$10^3 \times G_a(17,18^4)$		6.533(24)		
$10^7 \times Z_5(17,18^4)$		−4.17(25)		

[a] Quantities in parentheses correspond to 1σ from the least-squares fit, but the real uncertainties in the parameters are almost certainly larger. Parameters without an uncertainty were fixed at the indicated values.
[b] Ground state parameters are from Winnewisser et al. [5]. Their reported values [5] for H_{KJ} and H_{JK} were also used for the ground state (but not for the other states).

branches. Unresolved asymmetry doublets were generally fitted to the mean of the two calculated components. The fit also included the three excited state microwave transitions within the $4v_{18}$ state [7]. We found that the ground state rotational parameters of Winnewisser et al. [5] worked very well and so decided to leave these fixed in the fit. After some experimentation, we chose a set of 30 parameters to vary, and these are reported in Table 1. They include 9 parameters for v_{12}, 10 for v_{17}, 5 for $4v_{18}$, 4 for the v_{12}/v_{17} interaction, and 2 for the $v_{17}/4v_{18}$ interaction. We note that the $4v_{18}$ rotational parameters are mostly determined by the microwave data included in the fit.

A complete list with observed and calculated line positions is given in Table A-1 of the Appendix, and a list of calculated energy levels is given in Table A-2. The quality of the fit was very good, with a root mean square deviation of only about 0.00023 cm^{-1}. The parameters in Table 1 should offer a good description of v_{17} up to about $J = 46$ and $K_a = 20$, with the exception of the perturbed $K_a = 8$ and 14 levels discussed below (and even here the errors are less than 0.03 cm^{-1}). For the weaker v_{12} state, the effective coverage is up to about $J = 37$ and $K_a = 15$, but it is possible that we could have missed some small local perturbations involving other vibrational states. For the $4v_{18}$ state, the values in Table 1 are to some extent only fitting parameters since no infrared transitions involving this state were directly observed. Nevertheless, the values of these parameters seem reasonable (see Section 4.3 below) and we believe that they provide meaningful information about this state.

4. Discussion of vibrational interactions

4.1. The interactions between v_{12} and v_{17}

The largest vibrationally off-diagonal interaction considered here is the *a*-type Coriolis interaction between v_{12} and v_{17} represented by the parameter $G_a(12,17)$. Its value of 0.25 cm^{-1} implies a rather modest zeta parameter of $\zeta^a_{12,17} \approx 0.079$. Since levels of v_{12} and v_{17} with equal K_a values never approach each other closely, the effect of this interaction is mainly a generalized one. In isolated band fits, it would result in effective A rotational constants which were smaller than expected for v_{12} and larger for v_{17}. But since we explicitly include both states in our analysis, our (''deperturbed'') A constants for these two states are actually quite similar to each other and to the ground state value.

There are also some localized interactions between v_{12} and v_{17}. For example, one of the $K_a = 4$ levels of v_{12} crosses the lower $K_a = 1$ level of v_{17} between $J = 38$ and 39. This results in a small gap in the v_{17} $^rQ_0$ branch which is indicated with an asterisk in Fig. 2. Another more widespread perturbation involves a $\Delta K_a = \pm 2$ interaction. It most strongly affects the $K_a = 6$ levels of v_{12} and $K_a = 4$ levels of v_{17}, but also influences neighboring K_a levels. The v_{17} $K_a = 4$ levels are pushed up in energy by this interaction, while the v_{12} $K_a = 6$ levels are pushed down. Finally, the most obvious interaction between v_{12} and v_{17} involves the *b*-type Coriolis term with $\Delta K_a = \pm 1$. Levels of v_{17} with (J, K_a) lie *above* the levels of v_{12} with $(J, K_a + 1)$ for $K_a \leqslant 9$, but *below* them for $K_a \geqslant 10$. This has the effect that

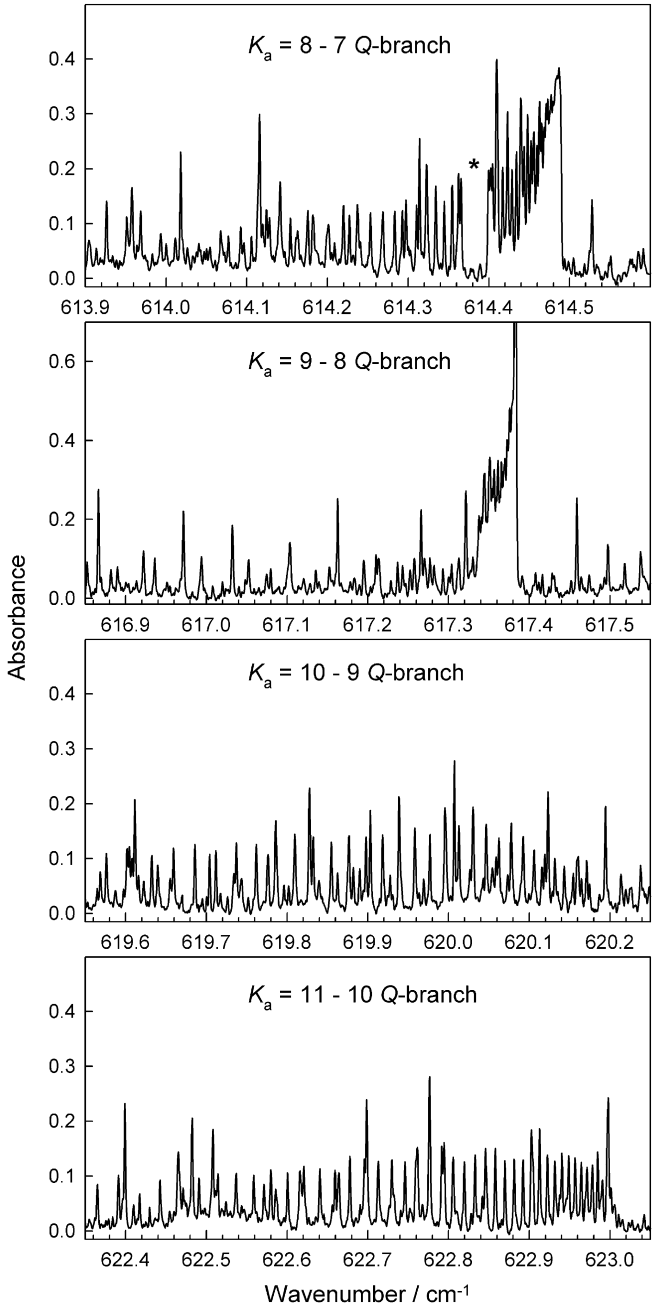

Fig. 4. Observed spectra of some ${}^{r}Q_{K_a}$ branches of the ν_{17} band of acrolein for $K'_a = 8$–11 (see also $K'_a = 7$ in Fig. 1). The dramatic change in the shape of these Q branches between $K'_a = 9$–10 is caused by the b-type Coriolis interaction with ν_{12} (see Section 4.1). The asterisk in the top panel indicates an unassigned local perturbation of the $K'_a = 8$ levels (see Section 4.3).

the ${}^{r}Q_{K_a}$ branches suddenly become more red-degraded for $K'_a = 10$ and higher, as illustrated in Fig. 4 (see also the $K_a = 7$–6 Q-branch in Fig. 1). A similar abrupt change is apparent in the ${}^{q}Q_{K_a}$ branch of the ν_{12} band, where the $K_a = 11$ sub-branch is blue-degraded while the sub-branches for other K-values tend to be red-degraded. This is somewhat apparent in Fig. 3 as a gap at 563.95 cm^{-1}, though it is masked by the general congestion in this region. This b-type Coriolis interaction between ν_{12} and ν_{17} was discussed by Hamada et al. [14]. In retrospect, their interpretation is mostly correct, but their description of a "split" in the ν_{17} ${}^{r}Q_9$ branch is not supported by our observations (see Fig. 4).

4.2. The interaction between ν_{17} and $4\nu_{18}$

As already mentioned above, the most obvious consequence of the interaction between ν_{17} and $4\nu_{18}$ occurs around $J' = 30$, $K'_a = 13$. This crossing of the $K_a = 13$ levels of ν_{17} and $4\nu_{18}$ causes a splitting in the ${}^{r}Q_{12}$ branch at 628.5 cm^{-1} which is illustrated in Fig. 5. This perturbation is also shown in Fig. 6, which shows residuals (observed minus calculated) for the ν_{17} $K_a = 13$ energy levels before (square points) and

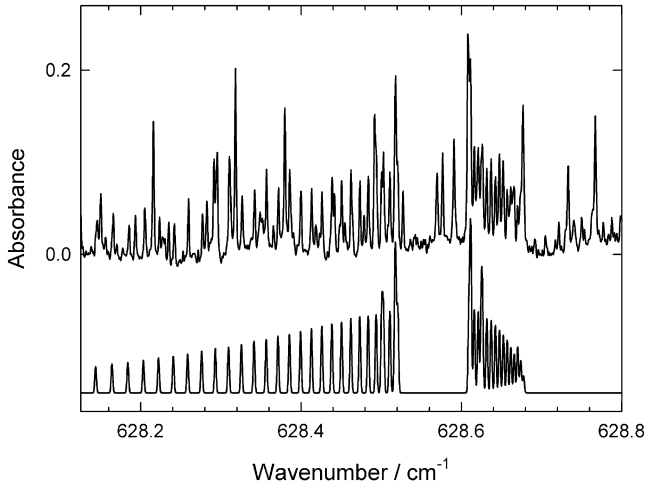

Fig. 5. The ${}^{r}Q_{12}$ branch of the ν_{17} band of acrolein, showing a perturbation of the ν_{17} state $K_a = 13$ levels around $J = 30$ by the $4\nu_{18}$ state. Upper trace: observed spectrum; lower trace: simulated spectrum.

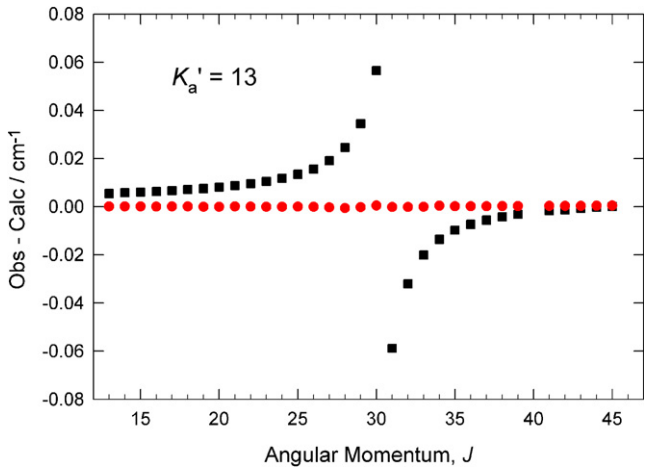

Fig. 6. Residuals (observed minus calculated) for the $K'_a = 13$ levels of the ν_{17} state illustrating a perturbation caused by the $4\nu_{18}$ state. The circular points are for the final fit, which explicitly included this interaction, and the square points are for an earlier fit which did not include the $4\nu_{18}$ state. (For interpretation of color mentioned in this figure the reader is referred to the web version of the article.)

after (round points) the perturbation had been properly accounted for by including the $4\nu_{18}$ state in the Hamiltonian.

It is legitimate to question how we can be sure that this perturbation of $K_a = 13$ levels is really due to $4\nu_{18}$, since rather similar (but unassigned) perturbations are also present at $K_a = 8$ and 14 (see Section 4.3 immediately below) and since no transitions involving $4\nu_{18}$ were directly observed. We believe that the assignment is justified by the fact that it fits the data almost perfectly, using parameters for $4\nu_{18}$ which are quite reasonable. Our value for the $4\nu_{18}$ origin, 622.0 cm^{-1} can be compared to the value of 624.0 cm^{-1} determined by Cole and Green [15] using contour simulations of hot bands in the torsional fundamental region ($\sim$160 cm^{-1}). Our values for the A, B, and C rotational constants of $4\nu_{18}$ are essentially determined by the excited state microwave transitions [7] included in the fit. We also determine a value for the distortion parameter Δ_K of $4\nu_{18}$ which is of opposite sign and larger in magnitude than the for ground state (see Table 1), and this may seem unreasonable at first. However, we have evidence from a preliminary unpublished analysis that the $2\nu_{18}$ state of acrolein at 314 cm^{-1} also has a negative Δ_K parameter, and we consider that $2\nu_{18}$ and $4\nu_{18}$ may be rather analogous. As well, there is a rather large correlation coefficient (0.969) between the $4\nu_{18}$ band origin and Δ_K values in our fit, so that, for example, values of $\nu_0 = 623.3$ cm^{-1} and $\Delta_K = -0.000035$ cm^{-1} result in only a small degradation in the quality of the fit.

4.3. Unassigned perturbations

In addition to the effects already noted, we observed two further local perturbations in the ν_{17} band which were not assigned. These occur around $(J, K_a) = (8, 40)$ and $(14, 33)$, and the former is visible in the top panel of Fig. 4, where a discontinuity in the $^rQ_7$ branch is indicated by an asterisk. In both cases, the correct perturbed level positions could be unambiguously determined by comparing the lines in the respective ^rQ and ^rP branches. The residuals between the observed and calculated levels are shown in Fig. 7. It is evident that the perturbations have similar magnitudes, and the same 'sign,' that is, in both cases the dark state has a larger effective rotational constant than ν_{17}. In our analysis, transitions of ν_{17} were given zero weight if they involved $K'_a = 8$, $J' > 33$, or $K'_a = 14$, $J' > 20$.

The culprits most likely responsible for these mystery perturbations are probably the $(\nu_{13} + 2\nu_{18})$ or $2\nu_{13}$ states, which are located at about 637.5 and 649.2 cm^{-1}, respectively, according to Cole and Green [15]. Other vibrational states that could conceivably be responsible are $3\nu_{18}$ at about 469.5 cm^{-1}, or $(\nu_{13} + \nu_{18})$ at about 484.1 cm^{-1} [15]. Approximate energy level calculations suggest that possible perturbers of ν_{17} at $K_a = 8$ are $K_a = 6$ or 5 of $(\nu_{13} + 2\nu_{18})$ or $2\nu_{13}$, respectively. In the case of ν_{17} at $K_a = 14$, the possible perturbers are $K_a = 13$ or 12, of $(\nu_{13} + 2\nu_{18})$ or $2\nu_{13}$, respectively. But at present we do not have sufficient evidence to make convincing choices among the various possibilities for these perturbations.

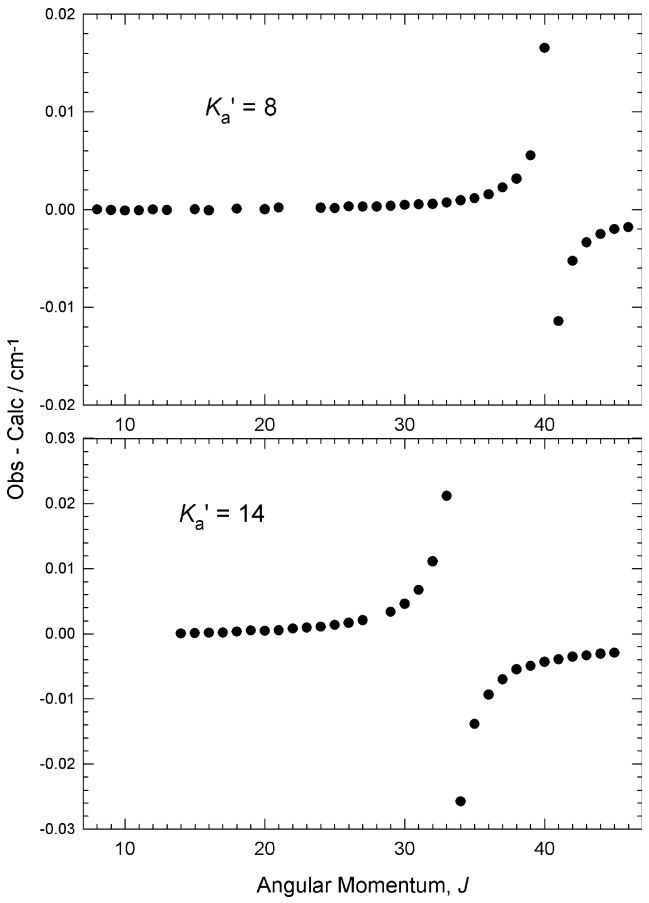

Fig. 7. Residuals (observed minus calculated) for the $K'_a = 8$ and 14 levels of the ν_{17} state illustrating two unassigned local perturbations. These are most likely caused by interactions with the $(\nu_{13} + 2\nu_{18})$ or $2\nu_{13}$ vibrational states (see Section 4.3).

5. Conclusions

The band origin values of 564 and 593 cm^{-1} reported earlier by Hamada et al. [14] for ν_{12} and ν_{17} agree very well with our new values of 564.340 and 593.079 cm^{-1}. As well, we agree with their conclusion, based on observation and theory, that ν_{12} is predominantly a-type, rather than b-type. All of the ν_{12} and ν_{17} rotational and centrifugal distortion parameters in Table 1 remain rather close to their respective ground state values. This tends to show that our analysis has accounted for all the important vibrational interactions and that there are no additional large systematic perturbations of these bands. On the other hand, a detailed analysis of the $4\nu_{18}$ state would probably have to take into account its interactions with the nearby $(\nu_{13} + 2\nu_{18})$ and $2\nu_{13}$ states, in addition to the interactions with ν_{17} and (indirectly) ν_{12} considered here.

In conclusion, we have used continuum infrared radiation from a synchrotron source, together with a Bruker IFS125 HR spectrometer, to study the ν_{12} and ν_{17}

fundamental bands of acrolein in the 550–650 cm^{-1} region with high spectral resolution (0.0012 cm^{-1}). The fit to the spectrum included almost 2000 lines and incorporated the *a*- and *b*-type Coriolis interactions between v_{12} and v_{17}, and well as an *a*-type Coriolis interaction with the $4v_{18}$ state which affects levels of v_{17} with $K_a \approx 13$. After the bands studied here, the next-strongest features in this spectral region are the hot bands originating from the first excited torsional level, $v_{18} = 1$, at 158 cm^{-1}, in particular the $(v_{17} + v_{18}) - v_{18}$ band whose origin is about 589 cm^{-1} [14]. It should be possible to perform a high resolution analysis of these bands analogous to that reported here for the fundamentals, but its scope might be limited by spectral congestion, particularly in the case of the more obscured $(v_{12} + v_{18}) - v_{18}$ hot band.

Acknowledgments

The research described in this paper was performed at the Canadian Light Source, which is supported by NSERC, NRC, CIHR, and the University of Saskatchewan. Financial support from the Natural Sciences and Engineering Council of Canada is gratefully acknowledged.

Appendix A. Supplementary data

Supplementary data for this article are available on ScienceDirect (www.sciencedirect.com) and as part of the Ohio State University Molecular Spectroscopy Archives (http://msa.lib.ohio-state.edu/jmsa_hp.htm).

References

[1] J.M. Hollis, P.R. Jewell, F.J. Lovas, A. Remijan, H. Møllendal, Astrophys. J. 610 (2004) L21–L24.
[2] H.E. Ayer, D.W. Yeager, Am. J. Public Health 72 (1982) 1283–1285.
[3] M.T. Borchers, S. Wesselkamper, S.E. Wert, S.D. Shapiro, G.D. Leikauf, Am. J. Physiol. Lung Cell. Mol. Physiol. 277 (1999) L489–L497.
[4] C.N. Harward Sr., W.D. Thweatt, R.E. Baren, M.E. Parrish, Spectrochim. Acta A 63 (2006) 970–980.
[5] M. Winnewisser, G. Winnewisser, T. Honda, E. Hirota, Z. Naturforsch. 30a (1975) 1001–1014.
[6] R. Wagner, J. Fine, J.W. Simmons, J.H. Goldstein, J. Chem. Phys. 26 (1957) 634–637.
[7] E.A. Cherniak, C.C. Costain, J. Chem. Phys. 45 (1966) 104–110.
[8] J.C.D. Brand, D.G. Williamson, Discuss. Faraday Soc. 35 (1963) 184–191.
[9] A.C.P. Alves, J. Christofferson, J.M. Hollas, Mol. Phys. 20 (1971) 625–644.
[10] E.J. Bair, W. Goetz, D.A. Ramsay, Can. J. Phys. 49 (1971) 2710–2717.
[11] G.A. Osborne, D.A. Ramsay, Can. J. Phys. 51 (1973) 1170–1175.
[12] K.W. Paulisse, T.O. Friday, M.L. Graske, W.F. Polik, J. Chem. Phys. 113 (2000) 184–191.
[13] R.K. Harris, Spectrochim. Acta 20 (1964) 1129–1141.
[14] Y. Hamada, Y. Nishimura, M. Tsuboi, Chem. Phys. 100 (1985) 365–375.
[15] A.R.H. Cole, A.A. Green, J. Mol. Spectrosc. 48 (1973) 232–245.
[16] B. Nelander, Vib. Spectrosc. 9 (1995) 29–41.
[17] M.S. Johnson, B. Nelander, Nuovo Cimento 20D (1998) 449–462.
[18] B. Nelander, V. Sablinskas, M. Dulick, V. Braun, P.F. Bernath, Mol. Phys. 93 (1998) 137–144.
[19] M.S. Johnson, F. Hegelund, B. Nelander, J. Mol. Spectrosc. 190 (1998) 269–273.
[20] J. Schroderus, V.-M. Hornemann, M.S. Johnson, N. Moazzen-Ahmadi, I. Ozier, J. Mol. Spectrosc. 215 (2002) 134–143.
[21] R. Wugt Larsen, F. Hegelund, B. Nelander, Mol. Phys. 102 (2004) 1743–1747.
[22] P. Roy, J.-B. Brubach, P. Calvani, G. deMarzi, A. Filabozzi, A. Gerschel, P. Giura, S. Lupi, O. Marcouillé, A. Mermet, A. Nucara, J. Orphal, A. Paolone, M. Vervloet, Nuclear Instruments and Methods in Physics Research, Section A 467–468 (2001) 426–436.
[23] J.K.G. Watson, in: J.R. Durig (Ed.), Vibrational Spectra and Structure, vol. 6, 1977, pp. 1–89.
[24] Y. Xu, J.W.C. Johns, A.R.W. McKellar, J. Mol. Spectrosc. 168 (1994) 147–157.
[25] http://physics.nist.gov/Divisions/Div844/facilities/uvs/jb95userguide.htm.